14th International Conference on Information Fusion
Chicago, Illinois, USA, July 5-8, 2011

Hierarchical Fusion Using Vector Quantization for Visualization of Hyperspectral Images

Parul Shah, Jayalakshmi M., Shabbir N. Merchant
Department of Electrical Engineering
IIT Bombay, India
Email: parul,jlakshmi,merchant@ee.iitb.ac.in

Uday B. Desai
Director
IIT Hyderabad,India
Email: ubdesai@iith.ac.in

Abstract— **Visualization of hyperspectral images that combines the data from multiple sensors is a major challenge due to huge data set. An efficient image fusion could be a primary key step for this task. To make the approach computationally efficient and to accommodate a large number of image bands, we propose a hierarchical fusion based on vector quantization and bilateral filtering. The consecutive image bands in the hyperspectral data cube exhibit a high degree of feature similarity among them due to the contiguous and narrow nature of the hyperspectral sensors. Exploiting this redundancy in the data, we fuse neighboring images at every level of hierarchy. As at the first level, the redundancy between the images is very high we use a powerful compression tool, vector quantization, to fuse each group. From second level onwards, each group is fused using bilateral filtering. While vector quantization removes redundancy, bilateral filter retains even the minor details that exist in individual image. The hierarchical fusion scheme helps in accommodating a large number of hyperspectral image bands. It also facilitates the midband visualization of a subset of the hyperspectral image cube. Quantitative performance analysis shows the effectiveness of the proposed method.**

Keywords: **Hierarchical fusion, hyperspectral imaging, image fusion, vector quantization, visualization.**

I. Introduction

Hyperspectral imagery produces images of a single scene taken at different narrow bands. These data are not exploitable in their original form, the different pieces of information contained in it have to be put together to be easily understandable. Hyperspectral sets of pictures show some specificities. They have a very high spectral resolution as the images are taken in very narrow bands. So the set of pictures has a very high redundancy due to the continuous bands registration of the sensors. The number of pictures describing a single scene is likewise bigger and lead to higher computational costs.

Some techniques used to answer this visualization problem analyze the set of pictures in order to select only several bands [1], or analyze the full set of pictures [2]. Recently, a visualization technique using bilateral filtering has been suggested in [3]. Authors claim that their method outperforms the previous work in literature. They performed a hierarchical fusion to answer to the high number of bands and reduce the computational time. The use of a bilateral filter preserves the edge while the finest features are removed.

Hyperspectral imagery produces images of the same area on the earth, taken at hundreds of continuous narrow-bands, covering the visible and the infrared wavelength spectra. These data are not exploitable in its original form; the different pieces of information contained in it have to be put together to be easily understandable. The hyperspectral data can be applied to studies in the field of remote sensing, environmental science, monitoring of environment hazards, geological surveying, agriculture, oceanology, volcanology and surveillance due to their distinct advantages in object characterization and identification. Hyperspectral images have a very high spectral resolution along with very high redundancy due to the contiguous narrow spectral bands of the sensors. The number of images describing a single scene is likewise bigger (usually 200 or more) and lead to higher computational costs and huge storage requirements.

II. Related Work

An efficient data fusion that can integrate data from multiple sensors, can be the solution to the hyperspectral image visualization. The research in the remote sensing image fusion can be broadly classified into two categories: multispectral (MS) and panchromatic (pan) image fusion and, multiband image fusion [3]. The pan-sharpening algorithms involve the extraction of high-resolution spatial data from pan images and merging them with MS images for sharpening. Various methods for achieving this task, known as pan-sharpening have been reported which include component substitution framework [4], intensity-hue-saturation (IHS) transformation [5], specific image formation model [6], etc. Methods based on multiresolution decomposition of spectral bands like wavelet packet transform based fusion [7] and contourlet transform based fusion [8] have also been suggested for pan-sharpening. A comparative analysis of image fusion methods is given in [9] and [10].

These techniques of musltispectral (MS) and panchromatic (pan) image fusion where the MS images with higher spectral resolution but lower spatial resolution are fused with the pan images of higher spatial but lower spectral resolution, are not suitable for hyperspectral image fusion [3] as here images are of the same spatial resolution. In [2], authors proposed a low complexity approach to generate a color display using three suitable image bands determined by 1-bit transform method. Jacobson *et al.* [1] introduced linear projection onto fixed basis functions, to reduce the dimensionality. But these methods

utilize only a few bands for visualization after analyzing the entire data sets. Exploiting all the bands, in [3], authors have proposed a visualization technique using bilateral filtering and a hierarchical fusion. They grouped contiguous bands uniformly with fixed group size at each level of hierarchy and then fused each group using bilateral filter. The use of a bilateral filter preserves the edges while the hierarchical fusion reduces the computational time. The method performs better compared to all other existing schemes [1], [2].

III. Hierarchical Fusion

A typical hyperspectral image data set in remote sensing contains a few hundred images to be fused into a single image (for grayscale) or three images (for RGB). Fusing all these given images together results in assigning very small fractional weights to the locations in each of the image bands. Moreover, some of these weights are comparable to the truncation errors, which is likely to wash out some of the minor details during fusion. Furthermore, all the images across all the bands, are needed for the computation of such fractional weights. Therefore, such fusion requires the entire hyperspectral cube to be read into memory. Considering the huge size of a hyperspectral image cube, the memory requirement goes over a few hundreds of megabytes.

In this paper, we advocate the use of hierarchical fusion with the help of vector quantization to overcome these issues. For the hyperspectral image cube of dimensions $(X \times Y \times N)$, containing N image bands, we apply the proposed vector quantization (VQ) based fusion across a contiguous subset of dimensions $(X \times Y \times P)$ to generate $B = N/P$ different fused images at the first stage of hierarchy as shown in Fig. 1. VQ helps in removing redundancies while retaining the features. In the subsequent levels of hierarchy, contiguous images are grouped together in a smaller subset and fused using 'bilateral filtering' described in section IV-A.

We perform uniform grouping followed by fusion till say J levels of hierarchy, to get a single fused image. By generating three fused images at the second last stage and assigning them to appropriate color channels, we can obtain the RGB representation of the fused hyperspectral image cube for the tristimulus visualization. This technique requires only P (or less) number of contiguous image bands for the fusion at a given stage. So the memory requirement significantly reduces as only P (or less) images out of N are read into memory at a time, which are typically less than 10% of the original number of image bands. The resultant fused images at the intermediate stages facilitate the visualization and analysis of the midband reflectance response of the scene.

IV. The Proposed Fusion using Vector Quantization based on LindeBuzoGray algorithm (LBG)

Vector quantization is a very powerful tool for image compression. The huge amount of data present in hyperspectral images remains a challenge in fusing these images. The high redundancy present in the hypercpectral data can be utilized to get a sparse representation using VQ. This section explains the approach of using LindeBuzoGray algorithm (LBG) [11] based VQ for image fusion.

Vector quantization is employed in Stage 1 of the proposed hierarchical fusion shown in Fig. 1. At the first stage of hierarchy, the images I_1 to I_N from N contiguous bands are organized into $Group1$ to $GroupB$, using uniform grouping. So each group has $P = N/B$ images each of size $X \times Y$. Each group is individually fused using VQ at the first stage of fusion.

As the first step of fusion, each image I_k is divided into sub-blocks of size $m \times m$ giving rise to $(X \times Y)/m^2$ image blocks. Thus in a given group, there are $IV_n = (X \times Y \times P)/(m^2)$ image sub- blocks. Convert these image vectors to 1-dimensional vectors each of size $1 \times m^2$ and generate a cluster (matrix) S of size $IV_n \times m^2$. Then the first code-vector ($CV^{(1,1)}$) of the code-book size 1, can be computed by finding the columnwise average of the entire cluster as follows:

$$CV^{(1,1)}(j) = \frac{1}{IV_n} \sum_{l=1}^{IV_n} S(l,j) \qquad 1 \leq j \leq m^2 \tag{1}$$

To double the code-book size, the code-vector ($CV^{(1,1)}$) is then split into two code-vectors by adding and subtracting a tolerance ϵ. In general, a code-vector can be represented as $CV_r^{(p,q)}$ where p represents the size of the code-book, q represents the code-vector's index within the code-book and r represents the iteration number.

$$CV_1^{(2,1)}(j) = CV^{(1,1)}(j) + \epsilon \tag{2}$$

$$CV_1^{(2,2)}(j) = CV^{(1,1)}(j) - \epsilon \tag{3}$$

Now the original cluster S is divided into two clusters namely $S1$ and $S2$ based on the distortion with respect to the code-vectors. The distortion $D_1^{(2,1)}$ and $D_1^{(2,2)}$ with respect to the code-vectors $CV_1^{(2,1)}$ and $CV_1^{(2,2)}$ respectively can be computed as follows:

$$D_1^{(2,1)}(k) = \frac{1}{m^2} \sum_{j=1}^{m^2} (CV^{(2,1)}(j) - S(k,j))^2 \tag{4}$$

$$D_1^{(2,2)}(k) = \frac{1}{m^2} \sum_{j=1}^{m^2} (CV^{(2,2)}(j) - S(k,j))^2 \qquad 1 \leq k \leq IV_n \tag{5}$$

Comparing the values $D_1^{(2,1)}(k)$ and $D_1^{(2,2)}(k)$ the image vectors of the cluster S is grouped into two sub-clusters $S1$ and $S2$ such that $S1 \bigcup S2 = S$ and $S1 \bigcap S2 = \Phi$.

$$If \quad D_1^{(2,1)}(k) < D_1^{(2,2)}(k); S(k,:) \subset S1 \qquad Else \quad S(k,:) \subset S2 \tag{6}$$

We now enhance the quality of the code-book by updating existing code-vectors through calculating the mean of the

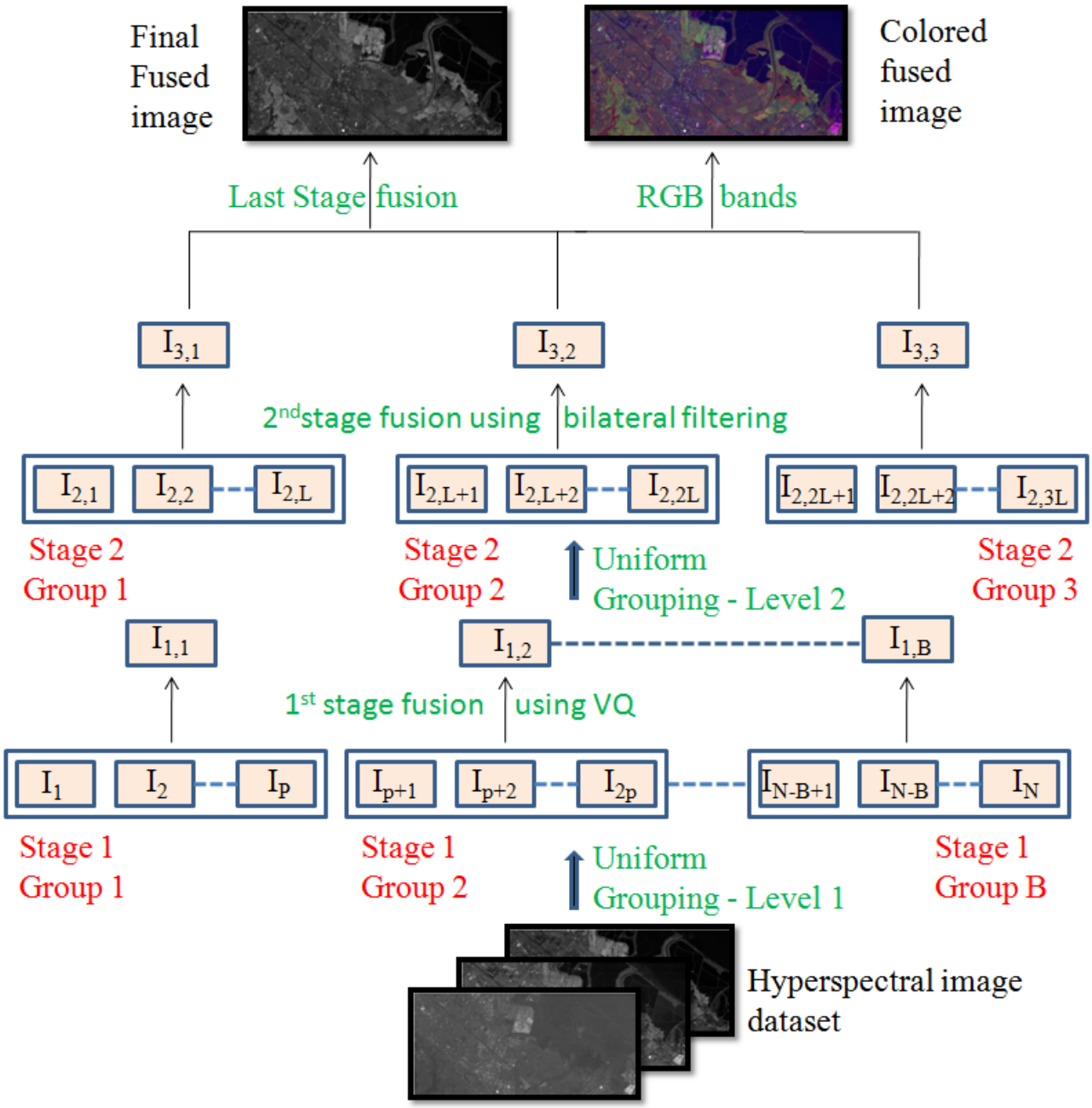

Fig. 1. Proposed scheme of the hierarchical (3 stage) fusion for the hyperspectral image cube.

image-vectors in each sub-cluster $S1$ and $S2$ as per Equation 1. The code-vectors $CV_1^{(2,1)}$ and $CV_1^{(2,2)}$ are updated to new code-vectors, say,$CV_2^{(2,1)}$ and $CV_2^{(2,2)}$. The corresponding distortions $D_2^{(2,1)}$ and $D_2^{(2,2)}$ are calculated for the complete image vector set S to get updated sub-clusters $S1$ and $S2$. The updation has to be repeated until the vector sum of the distortion in the $(r+1)^st$ level is significantly less than the distortion in the $(r)^th$ level, i.e. until $D_{(r+1)} << D_{(r)}$. At the end of last update, we get our final code-book of size 2.

This complete cycle can be repeated to double the code-book size further. To begin with the next cycle, the final code-vectors obtained at the end of the previous cycle, (e.g. $CV^{(2,1)}$ and $CV^{(2,2)}$ at the end of first cycle), are split on the same line as in 2. Thus number of code-vectors generated doubles in each cycle.

Let us assume that there are n code-vectors, each of size $1 \times m^2$, in the code-book (size $n \times m^2$). We have to fuse P images to a single image using this code-book. Let I_i represent the i^{th} image in a group and g_j^k represent the j^{th} sub-block (size $m \times m$) of the k^{th} image. We rearrange image I_i to $\widetilde{I}_i$ in a matrix of size $(X \times Y/m^2, m^2)$. So each $m \times m$ sub-block is rearranged as a row matrix (size $1 \times m^2$) in $\widetilde{I}_i$ and compared with all the n code-vectors with respect to MSE as follows.

$$MSE(i,j,k) = \frac{(CV^i - g_j^k)^2}{m^2} \quad (7)$$
$$where 1 \le i \le n$$
$$1 \le j \le (X \times Y)/m^2$$
$$1 \le k \le P$$

The MSE values of all the P images for a given sub-block position with all the code-vectors are then added. The code-vector CV^i that gives the minimum sum of MSE values is selected as the i^{th} sub-block of the fused image I_F as described by Equation 8. This is repeated for all the sub-blocks to get the fused image for a group.

$$If \sum_{k=1}^{P} MSE(m,j,k) \le \sum_{\forall i;k=1}^{P} MSE(i,j,k) \quad (8)$$
$$then \widetilde{I_F}^j = CV^m \quad (9)$$
$$\forall j$$

Thus at the end of first stage fusion, there are B fused images ($I_{1,1}$ to $I_{1,B}$) which are the input images for second level of hierarchy.

A. Fusion using Bilateral Filtering

In [3], authors propose to use bilateral filtering at every level of hierarchy for effective fusion of hyperspectral images. In the proposed method, bilateral filtering is used only from the second hierarchical level following the redundancy removal in the first stage through VQ.

Let I be the image to be processed using a bilateral filter. Let G_{σ_S} be the Gaussian spatial kernel, which is similar to traditional Gaussian filter. The value of σ_S decides the spatial extent of the kernel or the neighborhood under consideration. Let G_{σ_R}be the Gaussian range kernel, where σ_R decides the "amplitude" of the edge and its corresponding weight. The new value of pixel (x, y) of image I is obtained from pixels $(\widetilde{x}, \widetilde{y})$ in the neighborhood of the corresponding pixel as shown in the following:

$$I_{BF}(x,y) = \frac{1}{W(x,y)} \sum_x \sum_y G_{\sigma_S}(x - \widetilde{x}, y - \widetilde{y}) \quad (10)$$
$$\times G_{\sigma_S}(I(x,y) - I(\widetilde{x}, \widetilde{y}))I(\widetilde{x}, \widetilde{y})$$

Let $I(x, y, \lambda_1)$ to $I(x, y, \lambda_N)$ be the subset of a hyperspectral image cube, containing N images from consecutive wavelength bands λ_1 to λ_N. We calculate the weight at each pixel (x, y) for each image, w_1 to w_N, using the bilateral filter as follows:

$$w_i(x,y) = \frac{\mid I(x,y,\lambda_i) - IBF(x,y,\lambda_i) \mid + K}{\sum_{i=1}^{N} (\mid I(x,y,\lambda_i) - IBF(x,y,\lambda_i) \mid + K)} \quad (11)$$

where I_{BF} is the corresponding bilateral filtered image. A positive real number K allows flexibility in the fusion process by increasing or decreasing the effect of actual weight components and prevents numerical instability at homogenous regions. The fused image of the hyperspectral cube subset I_F is given by

$$I_F(x,y) = \sum_{i=1}^{M} wi(x,y) I(x,y,\lambda_i). \quad (12)$$

V. Hyperspectral Dataset

To test our grouping techniques algorithm, we have used hyperspectral urban data provided by the $Hyperion$ imaging sensor used in the EO-1 spacecraft for Earth observation(obtained from the US Geological Survey, http://eo1.usgs.gov) [12]. The data consists of 242 bands (0.4-2.5 μm) with 30-m spatial resolution. We have used the terrain-corrected data set (designated as Level G1), which is provided as 16-bit radiance values. The selected data set depicts the urban region of Palo Alto, CA (latitude: 37.4761^o N, longitude: 122.1341^o W). The dimension of the $Hyperion$ data cube is $(256 \times 512 \times 242)$.

The other set is the $Cuprite$ (cup95). It comes from the $AVIRIS$ sensor (Airborne Visible/Infrared Imaging Spectrometer) and was provided by the National Aeronautics and Space Administration/Jet Propulsion Laboratory (This data is downloaded from http://aviris.jpl.nasa.gov). It counts 50 pictures of size 400×350 pixels taken in the same bands between $0.4 - 2.5\mu m$.

These two sets have been chosen due to their different characteristics: cup95 counts fewer pictures with high similarity. $Hyperion$ counts more images which are distinctly different from each other in some areas.

(a) (b)

Fig. 2. The 1^{st} and the 81^{st} image of the urban image cube (Palo Alto) from $Hyperion$ dataset

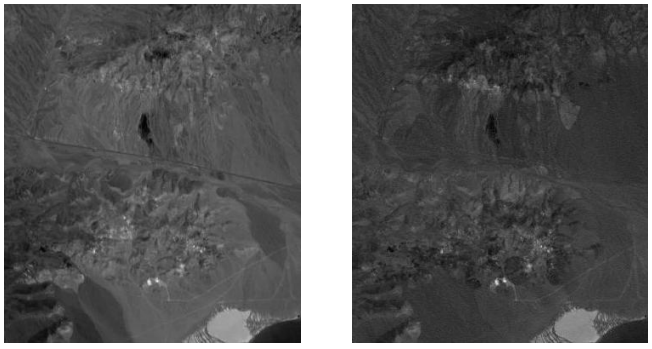

(a) (b)

Fig. 3. The 1^{st} and the 48^{th} image of the $Cuprite$ image cube ($cup95$) from $AVIRIS$ dataset

The contents of these data sets are also distinct. While $Hyperion$ data set highlights urban and vegetation features, $Cuprite$ emphasizes on geological features. We have tested on two more data sets provided by $AVIRIS$, namely $Moffett02$ and $Moffett03$, but have not reported their results here due to limited space.

VI. Quantitative Measures of Fusion Performance

Objective evaluation of fusion quality for the multiband image fusion in the absence of ground truth still does not have a universally accepted solution. The performance parameters for MS and pan image fusion have been reported in the literature [13]- [15], but these cannot be applied to the fusion schemes where reference image is not available. We present the performance evaluation of the proposed scheme on the basis of statistical assessment parameters given in [3], [6] and [16]. The entropy (H) of an image I can be considered as an index to evaluate the information content in the image and can be computed as follows.

$$H = -\sum_{i} p_I(i) ln(p_I(i)) \tag{13}$$

where p_I is the probability density of the intensity level i in the image. The average gradient $\bar{G}$ of an image is the measure of image sharpness in terms of gradient values. It can be computed as follows for an image I of size N.

$$\overline{G} = \frac{\sum_x \sum_y \sqrt{((I_{(x,y)} - I_{(x+1,y)})^2 + (I_{(x,y)} - I_{(x,y+1)})^2)}}{N} \tag{14}$$

This parameter has also been reported as the definition of an image in [16]. Besides these parameters, we also compute the standard deviation (SD or σ) which reflects the spread in the data and the average gray intensity value of the image (Mean or μ). Theoretically, for all these parameters, a higher value means better fusion quality. However, in presence of noise, image entropy as well as average gradient can be higher though the visual quality is poorer. So visual inspection is a must in such cases.

VII. Results and Analysis

We compare our results quantitatively in Table I with the most recently published method [3] based on hierarchical fusion using the bilateral filter. This method [3] has been proved to be superior to all other existing techniques like the three-band representation [1], the use of piecewise linear functions [1], the technique of the color matching functions [1], and the 1BT-based method [2]. Fig. 4 helps in the visual comparison of the fusion quality of the techniques.

The visualization results for the proposed approach and the reference approach [3] are shown in finer detail in Fig. 4 for $Hyperion$ dataset and in Fig. 5 for the $Cuprite$ hyperspectral image cube to visually inspect and compare the quality and sharpness of the fused images using the proposed method and the reference method. In these, Fig. (a) and (b) is result of hierarchy 15-3-1 i.e. 15 groups at the first stage and 3 groups at the second stage, which were fused to get the final fused image. Whereas, Fig. (c) is result of hierarchy 9-3-1. Different hierarchy combination with different number of stages can be tried and that can give different visualization results.

Fig. 6 and 7, show the fused images at intermediate level of hierarchy. Fig. 8 and 9 show colored fused image which can be obtained by having three groups at the second last stage generating three fused images, which can be used as R-G-B bands to display a colored fused image.

It is evident from these results that the fused images using the proposed method, are able to retain the textural details in the constituent bands very well. This is specifically so in the urban areas where the need to preserve the spatial details is very crucial. It can be seen that the result of the proposed

method not only provides sharp features but also preserves the finer details with accuracy. It also gives better contrast improving the visualization. Furthermore, the ringing artifacts and blurring of textures that appear in the fused images using wavelet-based approaches [10] are totally absent in the results of the proposed method.

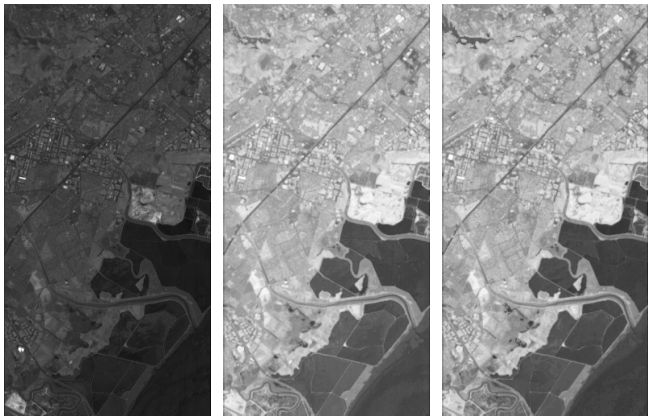

(a) (b) (c)

Fig. 4. Visual comparison of the performance of various image fusion approaches fusing the urban hyperspectral image cube (Palo Alto). Results of fusion using (a) $Bilateral$ filtering [3] with 15 groups at first stage and 3 groups at the second stage (b) the proposed method with 15 groups at first stage and 3 groups at the second stage (c) the proposed method with 9 groups at first stage and 3 groups at the second stage

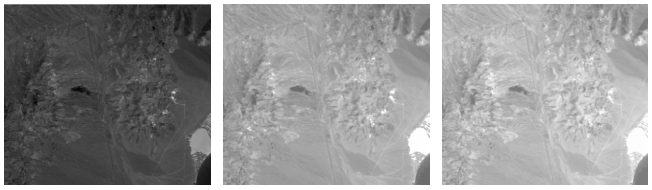

(a) (b) (c)

Fig. 5. Visual comparison of the performance of various image fusion approaches fusing the $Cuprite$ image cube. Results of fusion using (a) $Bilateral$ filtering [3] with 15 groups at first stage and 3 groups at the second stage (b) the proposed method with 15 groups at first stage and 3 groups at the second stage (c) the proposed method with 9 groups at first stage and 3 groups at the second stage

VIII. Conclusions

In this paper we have proposed a new approach for hierarchical fusion for efficient visualization of hyperspectral images. We use vector quantization for the first stage of fusion and bilateral filtering for the consequent stages. As redundancy is inherent to the hyperspectral data, vector quantization is helpful in reducing the same effectively. Once the redundancy is reduced, the bilateral filter based fusion retains all the minor details that exist in individual bands without introducing any blurring or ringing effect. As we are utilizing all the available bands for fusion, the loss of information is reduced

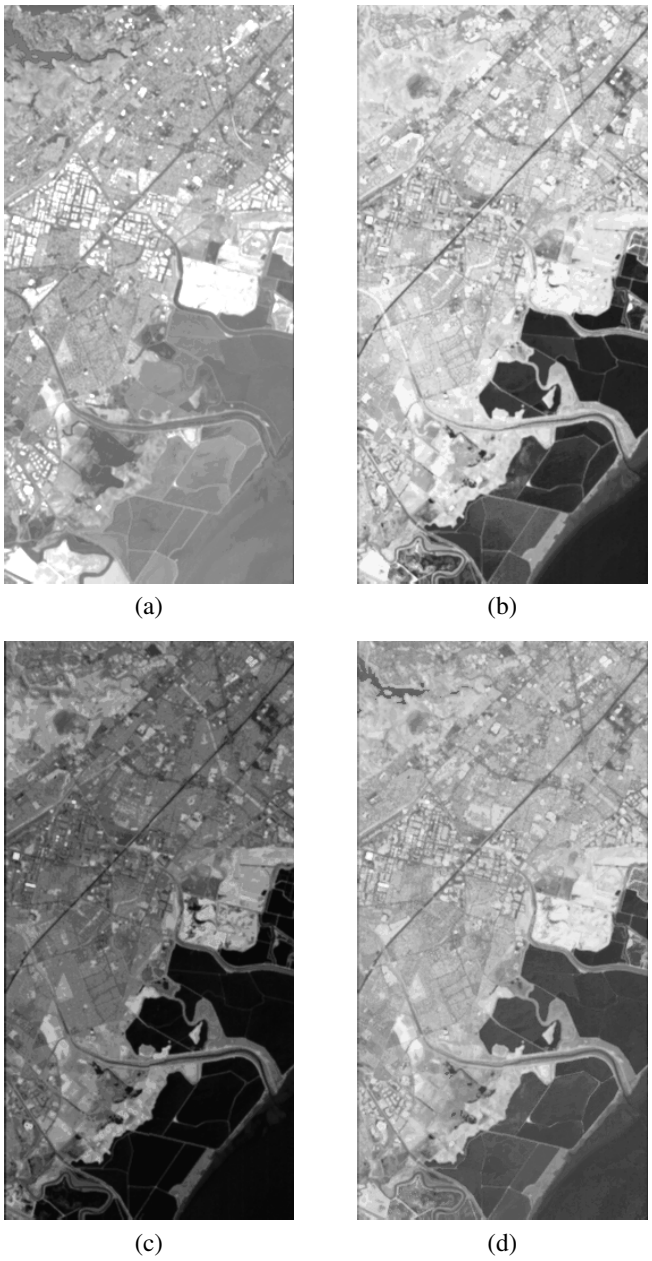

(a) (b) (c) (d)

Fig. 6. Results of the second-stage fusion of the urban image cube (Palo Alto) from $Hyperion$ data and the final fused image. These images are linearly scaled to the range [0, 255] for display purposes. (a) Fusion over bands 1–74 (b) Fusion over bands 75–154 (c) Fusion over bands 155–242 (d) Final fused image.

TABLE I

QUANTITATIVE PERFORMANCE EVALUATION

Fusion Method	Mean μ		SD σ		Entropy H		Avg Gradient $\bar{G}$	
	$Urban$	$Cuprite$	$Urban$	$Cuprite$	$Urban$	$Cuprite$	$Urban$	$Cuprite$
$Bilateral$ $15-3-1$ [3]	58.25	104.15	18.53	13.78	6.04	5.598	7.97	5.48
$Proposed$ $15-3-1$	**150.88**	164.82	45.16	19.8	7.18	6.06	11.98	5.537
$Proposed$ $9-3-1$	150.26	**185.06**	**47.26**	**20.08**	**7.21**	**6.23**	**12.77**	**6.09**

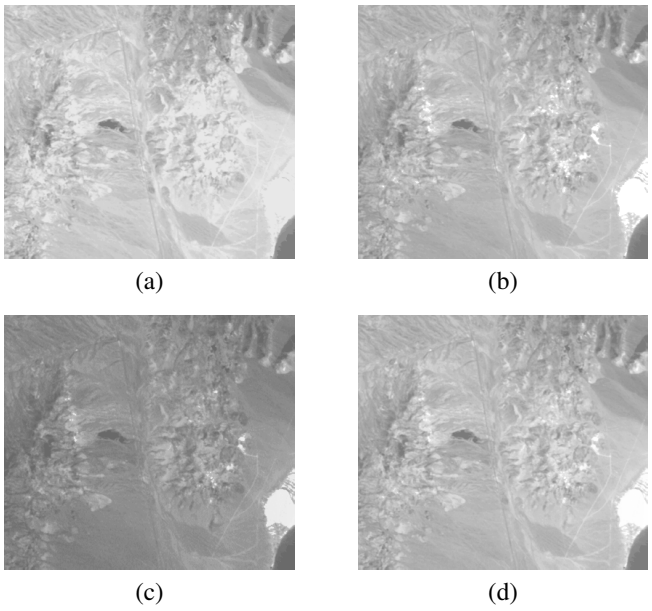

(a) (b) (c) (d)

Fig. 7. Results of the second-stage fusion of the $Cuprite$ image cube ($cup95$) from $AVIRIS$ dataset and the final fused image. These images are linearly scaled to the range [0, 255] for display purposes. (a) Fusion over bands 1–16 (b) Fusion over bands 17–32 (c) Fusion over bands 33–50 (d) Final fused image.

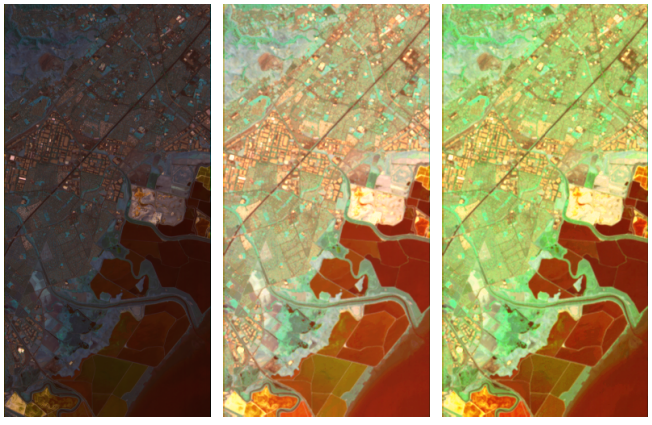

(a) (b) (c)

Fig. 8. Visual comparison of the performance of various image fusion approaches fusing the urban hyperspectral image cube (Palo Alto). Results of fusion using (a) $Bilateral$ [3] with hierarchy 15-3-1 i.e. 15 groups at first stage and 3 groups at the second stage (b) the proposed method with hierarchy 15-3-1 (c) the proposed method with hierarchy 9-3-1 after the tristimulus display of fused images shown in Fig. 6(a)(c).

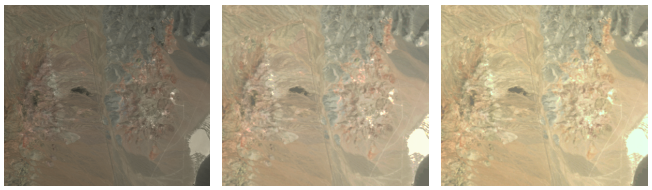

(a) (b) (c)

Fig. 9. Visual comparison of the performance of various image fusion approaches fusing the $Cuprite$ image cube. Results of fusion using (a) $Bilateral$ filtering [3] with hierarchy 15-3-1 i.e. 15 groups at first stage and 3 groups at the second stage (b) the proposed method with hierarchy 15-3-1 (c) the proposed method with hierarchy 9-3-1 after the tristimulus display of fused images shown in Fig. 7(a)(c).

significantly compared to the methods that use only three selected bands for visualization.

The performance of the proposed method have been compared with the best performing recent technique [3]. The proposed method outperforms the existing method visually as well as objectively in all the quantitative parameters. The major achievement is the significant improvement in standard deviation and average gradient values which makes the fused image sharper. The improved entropy indicates richer information content which is also evident from visual analysis. From the quantitative and visual analysis, it is clear that the proposed method displays the information content successfully in a colored image or gray image.

IX. ACKNOWLEDGEMENTS

This work was supported by Microsoft Research India under the MSRI PhD Fellowship Award 2008.

REFERENCES

[1] N. Jacobson, M. Gupta, and J. Cole, Linear fusion of image sets for display, *IEEE Trans. Geosci. Remote Sens.*, Vol. 45, No. 10, pp. 3277–3288, Oct. 2007.

[2] B. Demir, A. elebi, and S. Ertrk, A low-complexity approach for the color display of hyperspectral remote-sensing images using one-bittransform-based band selection, *IEEE Trans. Geosci. Remote Sens.*, vol. 47, no. 1, pp. 97–105, Jan. 2009.

[3] Ketan Kotwal and Subhasis Chaudhuri, "Visualization of Hyperspectral Images Using Bilateral Filtering," *IEEE Trans. on Geoscience And Remote Sensing*, Vol. 48, NO. 5, pp. 2308–2316, 2010.

[4] W. Dou, Y. Chen, X. Li, and D. Z. Sui, A general framework for component substitution image fusion: An implementation using the fast image fusion method, *Comput. Geosci.*, Vol. 33, No. 2, pp. 219–228, Feb. 2007.

[5] L. Alparone, L. Facheris, S. Baronti, A. Garzelli, and F. Nencini, Fusion of multispectral and SAR images by intensity modulation, in *Proc. 7th Int. Conf. Inf. Fusion*, Stockholm, Sweden, 2004, pp. 637–643.

[6] M. Joshi, L. Bruzzone, and S. Chaudhuri, A model-based approach to multiresolution fusion in remotely sensed images, IEEE Trans. Geosci. Remote Sens., Vol. 44, No. 9, pp. 2549–2562, Sep. 2006.
[7] W. Zhang and J. Kang, QuickBird Panchromatic and Multi-Spectral Image Fusion Using Wavelet Packet Transform, Vol. 344, *Lecture Notes in Control and Information Sciences*. Berlin, Germany: Springer-Verlag, 2006, pp. 976–981.
[8] V. Shah, N. Younan, and R. King, An efficient pan-sharpening method via a combined adaptive PCA approach and contourlets, *IEEE Trans. Geosci. Remote Sens.*, Vol. 46, No. 5, pp. 1323–1335, May 2008.
[9] Z. Wang, D. Ziou, C. Armenakis, D. Li, and Q. Li, A comparative analysis of image fusion methods, *IEEE Trans. Geosci. Remote Sens.*, Vol. 43, No. 6, pp. 1391–1402, Jun. 2005.
[10] L. Alparone, L. Wald, J. Chanussot, C. Thomas, P. Gamba, and L. Bruce, Comparison of pansharpening algorithms: Outcome of the 2006 GRS-S data-fusion contest, *IEEE Trans. Geosci. Remote Sens.*, Vol. 45, No. 10, pp. 3012–3021, Oct. 2007.
[11] Y. Linde, A. Buzo, R. M. Gray, "An Algorithm for Vector Quantizer Design," *IEEE Transactions on Communications*, Vol. 28, No. 1, pp. 84–94, Jan. 1980.
[12] D. Stein, J. Schoonmaker, and E. Coolbaugh, Hyperspectral imaging for intelligence, surveillance, and reconnaissance, *Space Naval Warfare Syst. Center*, San Diego, CA, Aug. 2001.
[13] C. Xydeas and V. Petrovic, Objective image fusion performance measure, *Electron. Lett.*, Vol. 36, No. 4, pp. 308–309, Feb. 2000.
[14] L. Wald, Quality of high resolution synthesized images: Is there a simple criterion? in *Proc. Int. Conf. Fusion Earth Data*, Sophia Antipolis, France, Jan. 2000, vol. 1, pp. 99–105.
[15] Z. Wang and A. Bovik, A universal image quality index, *IEEE Signal Process. Lett.*, vol. 9, no. 3, pp. 81–84, Mar. 2002.
[16] W. Cao, B. Li, and Y. Zhang, A remote sensing image fusion method based on PCA transform and wavelet packet transform, in *Proc. Int. Conf. Neural Netw. Signal Process.*, Nanjing, China, Dec. 2003, vol. 2, pp. 976981.